Available online at www.scholarsresearchlibrary.com

Scholars Research Library

Scholars Research Library

Annals of Biological Research, 2012, 3 (11):5350-5357
(http://scholarsresearchlibrary.com/archive.html)

Annals of Biological Research
Scholars Research Library
ISSN 0976-1233
CODEN (USA): ABRNBW

A biosensor by using Modified glassy carbon electrode With HRP Enzyme and Zro_2 Nanoparticles for Detect of H_2O_2

Mohamad Fazilati

Department of Biology, Payame Noor University, I.R. of IRAN

ABSTRACT

Design a biosensor by using Modified glassy carbon electrode With HRP Enzyme and Zro_2 Nanoparticles for Detect of H_2O_2 was studied. The heme group of HRP Enzyme played an important role in reduction (Fe^{2+}) an oxidation (Fe^{3+}) state in our electrochemical experiments. The phase characterization of ZrO_2 nanoparticles was performed by X-ray diffraction (XRD) using a D/Max-RA diffractometer with CuKα radiation. The absorbance properties of prepared nanoparticles were measured and recorded by using a TU-1901 double-beam UV-visible spectrophotometer. The morphologies and particle sizes of the samples were characterized by JEM-200CX transmission electron microscopy (TEM). The formal potential (E^0) for the HRP redox reaction on the HRP / ZrO_2 NPs/ GCE was equal to +0.49. This experiment has introduced a new biosensor for determination of H_2O_2 in the range of 50 to 400 μM.

INTRODUCTION

Nanomaterials are chemical substances or materials that are manufactured and used at a very small scale (down to 10,000 times smaller than the diameter of a human hair) [1-4]. Nanomaterials are developed to exhibit novel characteristics (such as increased strength, chemical reactivity or conductivity) compared to the same material without nanoscale features [5-6]. Nanomaterials have the potential to improve the quality of life; Metal nanoparticles (Nps) can be used to enhance the amount of immobilized biomolecules in construction of a sensor [7]. Metal nanoparticles have been used to catalyze biochemical reactions and this capability can be usefully employed in biosensor design. Nanotechnology is having a profound effect on the development of new biosensors. Biosensors commonly comprise a biological recognition molecule immobilised onto the surface of a signal transducer to give a solid state analytical device [8-9]. The reaction between the biorecognition molecule and the analyte is a heterogeneous reaction and therefore the design of the biosensing interface is all important in determining the final performance of the biosensor [10-11]. Advances in nanofabrication of biosensing interfaces are one of the two major areas where nanotechology has dramatically impacted on biosensor research in the last few years. The enzyme horseradish peroxidase (HRP), found in horseradish, is used extensively in biochemistry applications primarily for its ability to amplify a weak signal and increase detectability of a target molecule. Horseradish peroxidase is a 44,173.9-dalton glycoprotein with 6 lysine residues which can be conjugated to a labeled molecule. It produces a coloured, fluorimetric, or luminescent derivative of the labeled molecule when incubated with a proper substrate, allowing it to be detected and quantified [12]. HRP is often used in conjugates (molecules that have been joined genetically or chemically) to determine the presence of a molecular target [13]. The 3D structure of HRP was shown in figure 1. The heme group is clear in center of HRP structure with yellow color; this heme group played an important role in reduction (Fe^{2+}) an oxidation (Fe^{3+}) state in our electrochemical experiments [14].

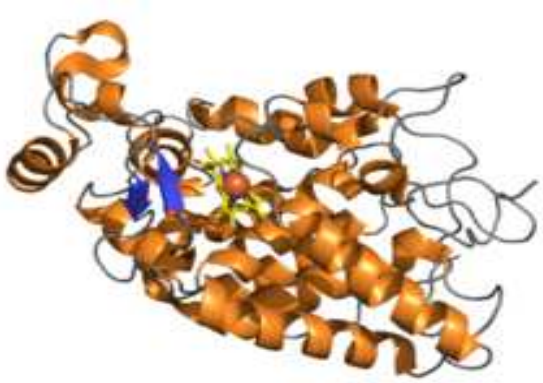

Figure 1. Three-dimensional structure of HRP.

Here we designed a biosensor by using Modified glassy carbon electrode With HRP Enzyme and Zro_2 Nanoparticles for Detect of H_2O_2.

MATERIALS AND METHODS

2.1. Materials

HRP and Zirconyl chloride octahydrate purchased from Sigma-Aldrich. Other Reagents purchased from Merck. The supporting electrolyte used for all experiments was 0.1 M pH 7 phosphate buffer solution (PBS), which prepared by using 0.1 M Na_2HPO_4 and NaH_2PO_4 solutions. All the reagents used were of analytical grade and all aqueous solutions were prepared using doubly distilled water generated by a Barnstead water system.

2.2. Apparatus

Cyclic voltammetry (CV) and square wave voltammetry were performed using an Autolab potentiostat PGSTAT 302 (Eco Chemie, Utrecht, The Netherlands) driven by the General purpose Electrochemical systems data processing software (GPES, software version 4.9, Eco Chemie). A conventional three-electrode cell was employed throughout the experiments, with bare or ZrO_2 nanoparticles modified glassy carbon electrode (3.0mm diameter) as a working electrode, a Ag/AgCl as a reference electrode, and a platinum electrode as a counter electrode. The phase characterization of ZrO_2 nanoparticles was performed by means of X-ray diffraction (XRD) using a D/Max-RA diffractometer with CuKα radiation. The absorbance properties of prepared nanoparticles were measured and recorded by using a TU-1901 double-beam UV-visible spectrophotometer. The morphologies and particle sizes of the samples were characterized by JEM-200CX transmission electron microscopy (TEM) working at 200 kV.

2.3. Preparation of ZrO_2 nanoparticles

The ZrO_2 nanoparticles were prepared according to the literature. Initially, 2.58 g $ZrOCl_2 \cdot 8H_2O$ and 4.80 g urea were dissolved in 20.0 mL CH_3OH under stirring to form a colorless solution. The solution was transferred to a 20-mL Teflon-lined stainless steel autoclave, which was heated to 200 °C and maintained at that temperature for 20 h. The obtained white product was post-treated with sulphuric acid solution (0.16 mmol), and then calcined at 645 °C.

2.4. Preparation of unmodified glassy carbon electrode

The most commonly used carbon-based electrode in the analytical laboratory is glassy carbon (GC). It is made by pyrolyzing (Pyrolysis is the decomposition of organic compounds by heating to high temperatures in the absence of oxygen) a carbon polymer, under carefully controlled conditions, to a high temperature like 2000°C [15]. An intertwining ribbon-like material results with retention of high conductivity, hardness, and inertness. Glassy carbon electrode (GCE, dia. 3mm) was polished with 1 μm and 0.05 μm alumina slurries sequentially and then rinsed with distilled water. After that, the electrode was sonicated in deionized water and finally dried under ambient conditions.

2.5. Preparation of modified GCE with ZrO_2 Nanoparticles and HRP

To prepare the modified GCE with ZrO_2 Nanoparticles and HRP, after immobilized ZrO_2 Nanoparticles on GCE surface, The ZrO_2 Nanoparticles / GCE was placed into a fresh PBS including 12mg mL^{-1} HRP (pH 7.0, 3 to 5°C) for 8 hour. At the end, the modified electrode was washed with deionized water and placed in PBS (PH 7.0) at a refrigerator (3 to 5°C), before being employed in the electrochemical measurements as the working electrode.

RESULTS AND DISCUSSION

3.1. Microscopic characterization

The average diameter of the Synthesized ZrO_2 nanoparticle is about 20 nm, and has a very narrow particle distribution. The scale bare for this image also was 20 nm. This statement illustrated in figure 2. This Figure Show a TEM picture of the ZrO_2 nanoparticles.

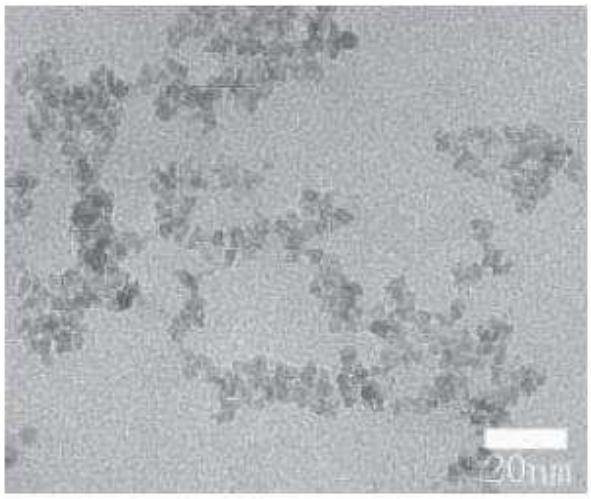

Figure 2. TEM images of ZrO_2 NPs, with diameter about 20 nm

3.2. X-Ray diffraction of ZrO_2 nanoparticles

The XRD pattern (figure 3) for ZrO_2 nanoparticles, the diffraction peaks are absorbed at 2θ values. The prominent peaks have been utilized to estimate the grain size of sample with the help of Scherrer equation [16] $D = K\lambda/(\beta \cos \theta)$ where K is constant(0.9), λ is the wavelength(λ = 1.5418 A°) (Cu Kα), β is the full width at the half-maximum of the line and θ is the diffraction angle. The grain size estimated using the relative intensity peak for ZrO_2 nanoparticles was found to be 20 nm and increase in sharpness of XRD peaks indicates that particles are in crystalline nature. All different peaks in figure 3 related to ZrO_2 nanoparticles and matched to Joint Committee for Powder Diffraction Studies (JCPDS).

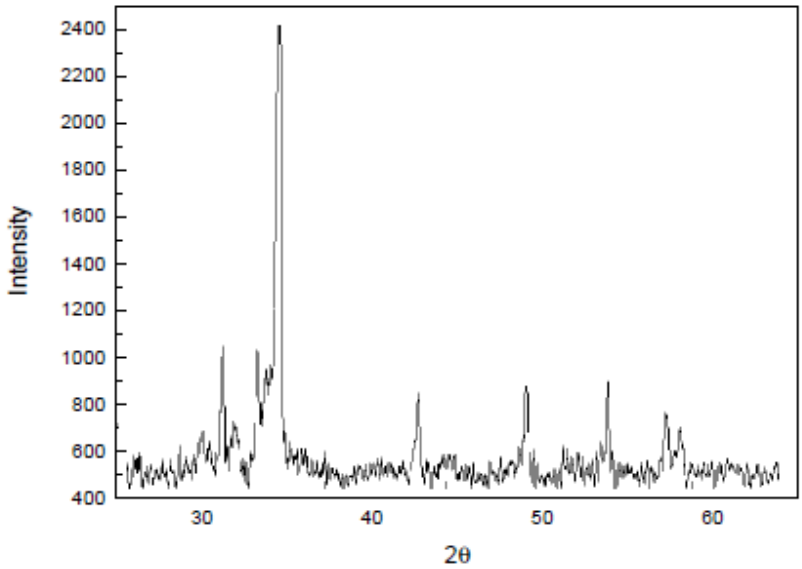

Figure 3. XRD pattern for ZrO_2 nanoparticles

3.3. UV–visible absorption spectra for ZrO_2 nanoparticles

The most dramatic property of nanoparticles is the size evolution of the optical absorption spectra. Hence UV-visible absorption spectroscopy is an efficient technique to monitor the optical properties of quantum-sized particles. The UV–visible absorption spectra of ZrO_2 nanoparticles was shown in Figure 4; although the wavelength of our spectrometer is limited by the light source, the absorption band of the ZrO_2 nanoparticles have been shows a blue shift due to the quantum confinement in sample compare with bulk ZrO_2 particles. This optical phenomenon indicates that these nanoparticles show quantum size effect [17].

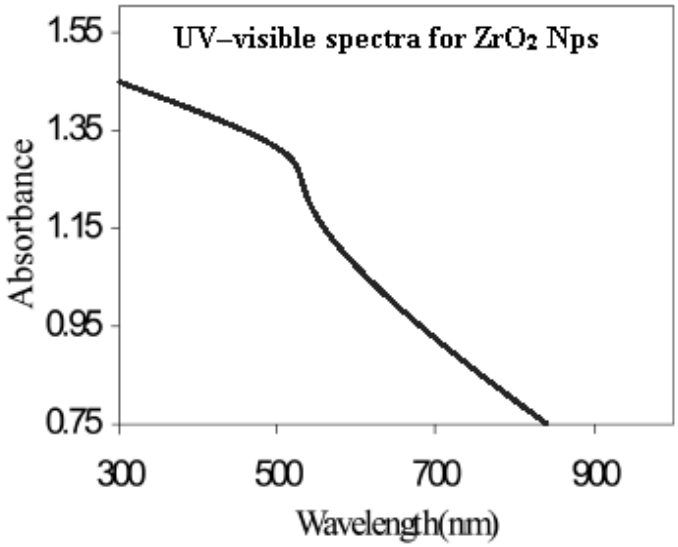

Figure 4. UV-Vis absorption spectra for ZrO_2 nanoparticles.

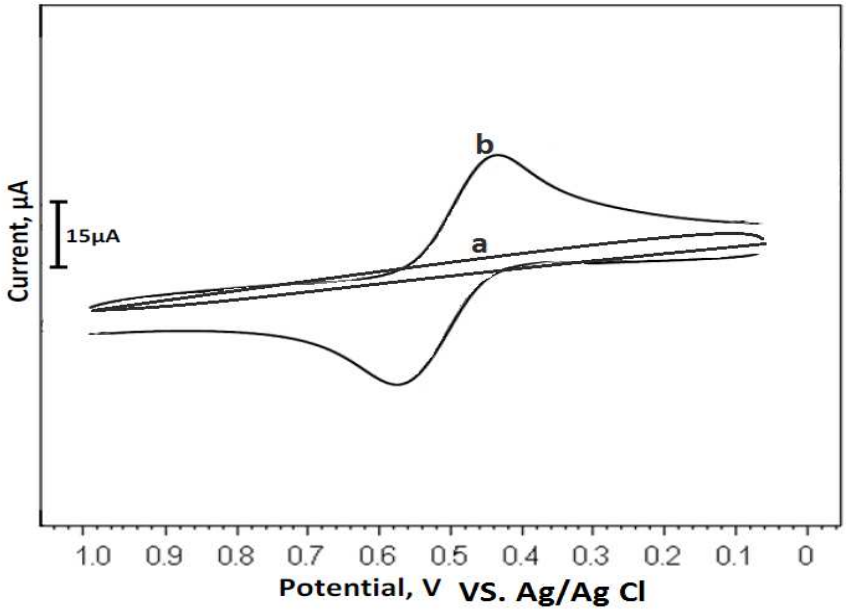

Figure 5. Cyclic voltammograms, using (a) the ZrO_2 NPs/ GCE in 0.1 M phosphate buffer and (b HRP / ZrO_2 NPs/ GCE in 0.1 M phosphate buffer (scan rate: 100 mV/s).

3.4. Direct voltammetric behavior of the HRP / ZrO_2 NPs/ GCE electrode

The integrity of the immobilized HRP construction and its ability to exchange electrons with the nanometerscale ZrO_2 particles surfaces were assessed by voltammetry. A macroscopic electrode was required to attain a large enough HRP sample to yield detectable direct oxidation and reduction currents. The comparative CVs for the ZrO_2

NPs/ GCE and HRP / ZrO_2 NPs/ GCE in 0.1 M PBS (pH 7.0) was obtained. These voltammograms are demonstrated in Figure. 5 (a,b). From this Figure, it was noticed that there were no voltammetric response on ZrO_2 NPs/ GCE (Fig. 5a), which, Fig. 5(b) depicts a well-defined pair of oxidation–reduction (redox) peaks, observed on the HRP / ZrO_2 NPs/ GCE at 100 mV s^{-1} scan rate value. The HRP / ZrO_2 NPs/ GCE presented the reductive peak potential at +0.42 V and the corresponding oxidative peak potential at +0.56 V (at 100 mV s^{-1}), illustrating the adsorbed HRP on the nanometer-scale ZrO_2 particle surfaces. The difference of anodic and cathodic peak potential values was ΔE = -0.14 V. These redox peaks were attributed to the redox reaction of the HRP electroactive center. The formal potential (E^0) for the HRP redox reaction on the HRP / ZrO_2 NPs/ GCE was +0.49 with respect to the reference electrode.

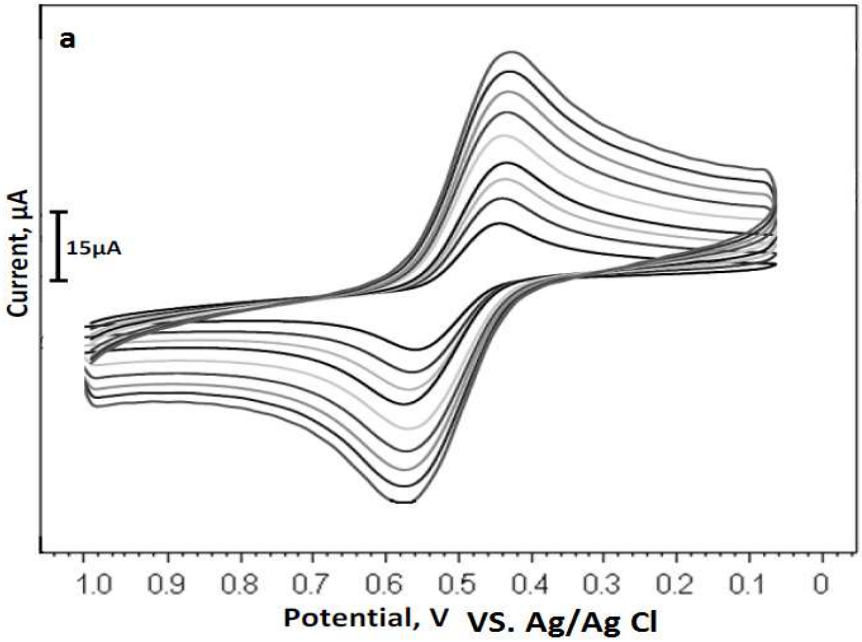

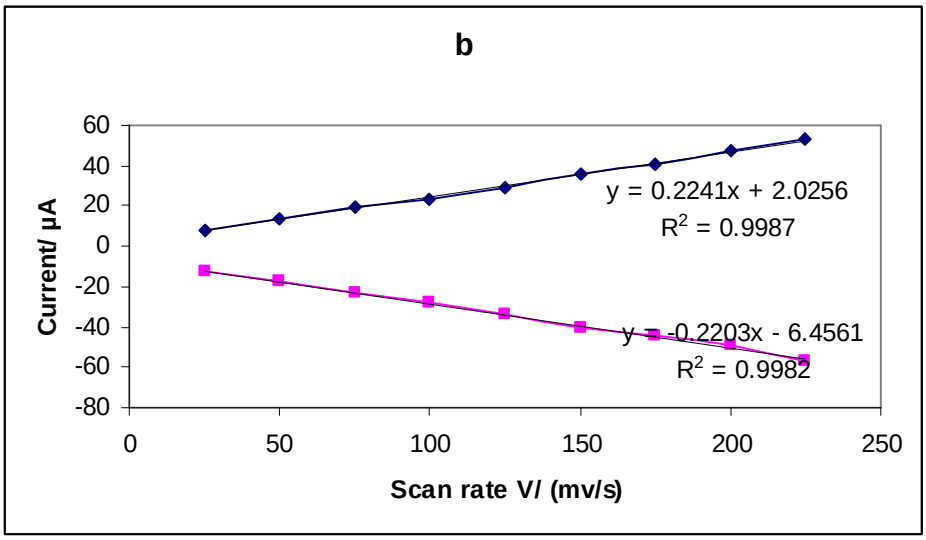

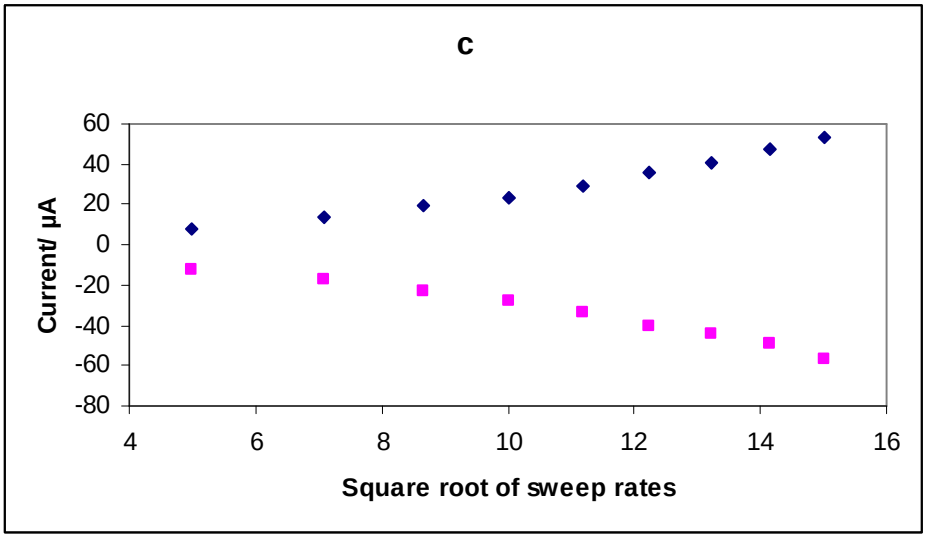

Figure 6. (a) CVs of HRP / ZrO_2 NPs/ GCE electrode in PBS at various scan rates, from inner to outer; 25, 50, 75, 100, 125, 150, 175, 200 and 225 mV s^{-1}, the relationship between the peak currents (ipa, ipc) vs., (b) the sweep rates and (c) the square root of sweep rates.

The collected voltammograms in Figure 6 (a) substantiated this statement that the nanometer-scale ZrO_2 particles could play a key role in the observation of the HRP CV response. On the grounds that the surface-to volume ratio increases with the size decrease and because of the fact that the enzyme size is comparable with the nanometer-scale building blocks, these nanoparticles displayed a great effect on the electron exchange assistance between HRP and GCE. To further investigate the HRP characteristics at the HRP / ZrO_2 NPs/ GCE electrode, the effect of scan rates on the HRP voltammetric behavior was studied in detail. The baseline subtraction procedure for the cyclic voltammograms was obtained in accordance with the method reported by Bard and Faulkner [18]. The scan rate (ν) and the square root scan rate ($\nu^{1/2}$) dependence of the heights and potentials of the peaks are plotted in Figure 6 (b) and Figure 6 (c) respectively. It can be seen that the redox peak currents increased linearly with the scan rate, the correlation coefficient was 0.9987 (ipc = +0.2241ν + 2.0256) and 0.9982 (ipa = -0.2203ν-6.4561), respectively. This phenomenon suggested that the redox process was an adsorption-controlled and the immobilized HRP was stable. In Figure 6 (c) It can be seen that the redox peak currents increased more linearly with the ν in comparison to that of $\nu^{1/2}$.

However, there is clearly a systematic deviation from linearity in this data, i.e. low scan rates are always on one side of the line and the high scan rate points are on the other. The anodic and cathodic peak potentials are linearly dependent on the logarithm of the scan rates (ν) when ν > 200 mV s^{-1}, which was in agreement with the Laviron theory, with slopes of -2.3RT/ α nF and 2.3RT/ (1 -α) nF for the cathodic and the anodic peak, respectively [19]. So, the charge-transfer coefficient (a) was estimated as 0.39. Furthermore, the heterogeneous electron transfer rate constant (ks) was estimated according to the following equation [19-20]:

$$[\log ks = \alpha \log(1-\alpha) + (1-\alpha)\log\alpha - \log\frac{RT}{nF\nu} - \frac{\alpha(1-\alpha)nF\Delta EP}{2.3\,RT}] \quad (1)$$

Here, n is the number of transferred electrons at the rate of determining reaction and R, T and F symbols having their conventional meanings. The average heterogeneous transfer rate constant (ks) value was calculated about, 1.81 s^{-1}.

3.5. Electrocatalytic reduction of H_2O_2 on the HRP / ZrO_2 NPs/ GCE

Upon addition of H_2O_2 to 0.1M pH 7.0 PBS, the cyclic voltammogram of the HRP / ZrO_2 NPs/ GCE electrode for the direct electron transfer of HRP changed dramatically with an increase of reduction peak current and a decrease of oxidation peak current (Fig. 7a), while the change of cyclic voltammogram of bare or ZrO_2 Nps/ GCE was negligible (not shown), displaying an obvious electrocatalytic behavior of the HRP to the reduction of H_2O_2. The decreases of the oxidative peak current together occurred with the increases of the reductive HRP / ZrO_2 NPs/ GCE. The electro-catalytic process could be expressed as follows:

$H_2O_2 + HRP_{red} \rightarrow HRP_{ox} + H_2O$ (2)

$HRP_{ox} + 2\ e^- \rightarrow HRP_{red}$ (3)

The calibration curve (Figure 7b) shows the linear dependence of the cathodic peak current on the H_2O_2 concentration in the range of 50 to 400 µM. In Figure 7 b, at higher concentration of H_2O_2, the cathodic peak current decreased and remains constant. Upon addition of an aliquot of H_2O_2 to the buffer solution, the reduction current increased steeply to reach a stable value (Fig 7 b). This implies electrocatalytic property of electrode. Thus, this experiment has introduced a new biosensor for the sensitive determination of H_2O_2 in solution.

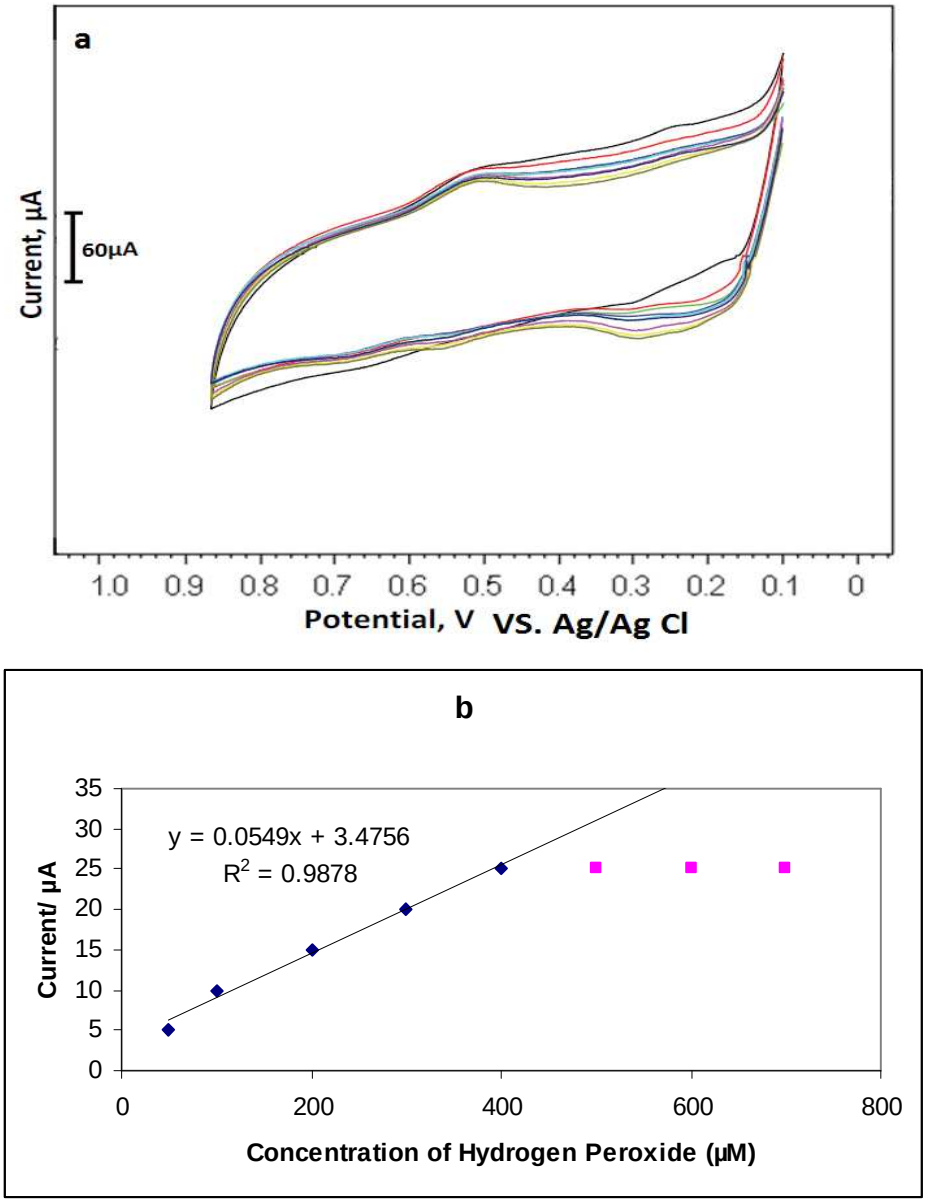

Figure 7. (a) Cyclic voltammograms obtained at an HRP / ZrO_2 NPs/ GCE in 0.1M PBS (pH 7.0) for different concentrations of H_2O_2 and (b) the relationship between cathodic peak current of HRP and different concentrations of H_2O_2 (scan rate: 100 mVs^{-1}).

3.6. Stability of designed H_2O_2 biosensor

The stability of H_2O_2 biosensor has been checked by carrying out experiments at the regular interval of a week and it has been found that HRP / ZrO_2 Nps/ GCE electrode based electrochemical biosensor retains its 92% activity after

30 days. The loss in the activity of biosensor is not due to the denaturation of HRP but it is due to the poor adhesion of ZrO_2 Nanoparticles on the GCE.

CONCLUSION

Nanotechnology is having a profound effect on the development of new biosensors. In this paper, i have constructed for design a new biosensor for the sensitive determination of H_2O_2 in solution. The H_2O_2 biosensor had successfully demonstrated high stability, good linearity, better sensitivity, fast response time, and excellent selectivity towards H_2O_2.

REFERENCES

[1] M. J. Sailor and J. R. Link, *Chemical Communications*, **2005**, 11, 1375–1383.
[2] V. Shah and I. Belozerova, *Water, Air, and Soil Pollution*, **2009**,197, 143–148.
[3] W.-X. Zhang, *Journal of Nanoparticle Research*, **2003**, 5, 323–332.
[4] D. W. Galbraith, *Nature Nanotechnology*, **2007,** 2, 272–273.
[5] Kress-Rogers, E. *Handbook of Biosensors and Electronic Noses*; CRC Press Inc.: New York, **1997**.
[6] Wise, D.L. *Bioinstrumentation and Biosensors*; Marcel Dekker: New York, **1991**.
[7] Turner, A.P.F.; Karube, I.; Wilson, G.S. *Biosensors Fundamentals and Applications*; Oxford Univeristy Press: Oxford, **1987**.
[8] Emanuel, P.A., Dang, J., Gebhardt, J.S., Aldrich, J., Garber, E.A.E., Kulaga, H., Stopa, P, Valdes, J.J., and Dion-Schultz, A, *Biosens. Bioelectron*, **2000**, 14, 751–759.
[9] Subrahmanyam, S., Piletsky, S.A., and Turner, A.P.F, *Anal. Chem*, **2002**, 74, 3942–3952.
[10] B. Wang, B. Li, Q. Deng, and S. Dong, *Analytical Chemistry*, **1998**, 70, 3170–3174.
[11] M. H. Yang, Y. H. Yang, Y. L. Liu, G. L. Shen, and R. Q. Yu, *Biosensors and Bioelectronics*, **2006**, 21, 1125–1131.
[12] Carlsson GH, Nicholls P, Svistunenko D, Berglund GI, Hajdu J. *Biochemistry*, **2005,** 44, 635–642.
[13] Veitch NC. *Phytochemistry*, **2004**, 65, 249–259.
[14] Chau YP, Lu KS. *Acta Anat (Basel)*, **1995**, 153, 135–144.
[15] D. T. Fagan, I-F Hu, T. Kuwana, *Anal. Chem*, **1985**, 57, 2759.
[16]H. Fan, L. Yang, W. Hua et al., *Nanotechnology*, **2004**, 15, 37.
[17]Jeremy Ramsden, *Essentials of Nanotechnology*, Ventus Publishing ApS. **2009**.
[18] A.J. Bard, L.R. Faulkner, *Electrochemical Methods*, second. ed., Fundamentals and Applications, Wiley, NY, **2001**, 241.
[19] E. Laviron. *Journal of Electroanalytical Chemistry*., **1979**, 101, 1, 19-28.
[20] E. Laviron. *Journal of Electroanalytical Chemistry*., **1979**, 100, 263-270.